FLUID FLOW AROUND A BLUFF-BODY INSIDE A LPP COMBUSTION CHAMBER - ISOTHERMAL FLOW

Luciano G. Noleto, Fabiano A. dos Santos, Antonio C. P. Brasil Junior, Armando Caldeira-Pires.
Universidade de Brasília. Departamento de Engenharia Mecânica.
LEA - Laboratório de Energia e Ambiente.
70910-900 Brasília. DF. Brazil.
E-mail: brasiljr@unb.br

Abstract: *The purpose of this paper is to present numerical results of the isothermal flow inside a LPP combustion chamber, for nonswirling and swirling cases. The simulation is based in the resolution of transient transport equations using the CFX 5.5.1 commercial software with a finite volume formulation. The geometry used was inspired in a LPP chamber which is going to be built in the combustion and propulsion laboratory of LEA. Visual results were obtained, and they show some agreement with experimental results, being fitted in flow patterns there were experimentally determined. The efficacy of the turbulence model, which were used in the simulation was investigated, and its possible flaws were discussed.*

Keywords: *Bluff-Body. Turbulence models. LPP Combustion Chamber.*

1. Introduction

A common feature of all the dry low NOx combustors is that positive efforts are made to eliminate local regions of high temperature within the flame by mixing the fuel and air upstream of the combustion zone. The lean, premix, prevaporize (LPP) concept represents the ultimate in this regard. Its underlying principle is to supply the combustion zone with a completely homogeneous mixture of fuel and air, and then to operate the combustion zone at an equivalence ratio which is very close to the lean blowout limit. The smaller the margin between stable combustion and flame blowout, the lower will be the output of NOx. A typical LPP combustor can be divided into three main regions (Fig. 1). The first region is for fuel injection, fuel vaporization, and fuel-air mixing. Its function is to achieve complete evaporation and complete mixing of fuel and air before combustion. In the second region the flame is stabilized by the creation of one or more recirculation zones. Combustion is completed in this region and the resulting products then flow into region three which may comprise a fairly conventional dilution zone.

The recirculation zone and the toroidal vorticity in any combustion chamber (in particular in the LPP chambers) provide great influence in the combustion. This phenomenon is responsible for the air/fuel mixture, since the holding and stability of the flame, and the mixing itself vary with the degree of turbulence in the free shear layers. The recirculation zones, inside chambers, can be obtained by swirlers, bluff-bodies or both of them. Specifically for the LPP chambers, the stability of the flame, inside the combustion chamber, can prevent most of the problems in this kind of combustor. The process of flame anchoring, provided by the flow around the bluff-body and the swirl, is the aim of the present study.

There have been many studies concerning the aerodinamical effects of bluff-bodies and swirlers in the structure of the flow. For instance, Taylor and Whitelaw(1984) studied the velocity behind some types of bluff bodies, and their conclusion is, the more the blockage ratio increases, the narrower and more lengthened the recirculation bubble becomes. Chigier and Beér(1964) measured velocity and pressure in an unconfined swirling annular jet and they varied the degree of swirl. They concluded that the formation of a closed toroidal vortex behind the central bluff body, and the strength and size of the vortex are affected by the variation of the swirl strength. Sheen et all. had visualized unconfined and confined annular swirling jets and studied the dynamic behaviors of the recirculation zone behind an axissymetric bluff body, and they concluded that exists seven different flow patterns: stable flow, vortex shedding, transition, prepenetration, penetration, vortex breakdown and attachment. This patterns are distinguished by the swirl number and the Reynolds number. They were able to give a relationship between the recirculation length and the swirl number. Huang and Tsai(2001) had shown the flow patterns of a swirling jet around various circular disks, concluding that, depending of the blockage ratio and the degree of swirl, the swirling-jet, weak-blockage-effect and bluff-body-effect regimes can be seen. The swirling-jet regime has the common behavior of the standard swirling jet, the weak-blockage-effect regime has the formation of a swirling wake, and the bluff-body-effect regime has a dual-ring bubble structure behind the disk. Also, in this regime, the following types of flow has been identified: a pair of counter-rotating vortex rings and a central swirling jet. Schefer et all(1994) had made velocity measures in a turbulent buff-body stabilized flow,

showing that, in a low inlet velocity ratios, the flow is dominated by the reverse flow of the annular air stream, exhibiting well-defined fuel jet and annular stagnation points along the centerline. Increasing the velocity ratio causes the increase of the fuel-jet penetration until the dynamic pressure of the jet is enough to surpass the adverse pressure gradient of the outer air, making the fuel jet penetrates the recirculation zone. Departures of isotropy were found in regions of high shear where the fluctuation of the axial component of the velocity is a factor of 2 greater than the radial component. Koutmos and McGuirk(1991) made a computational study of a gas turbine combustor using the $k-\epsilon$ model in order to validate it to the case, and, despite of its deficiencies, like the failing on predicting regions of strong anisotropy, the model can give reasonable results. Chen et all(1990) had compared stabilized flames with swirlers and bluff-bodies in industrial burners, and they also investigate the sources of the vorticity within the recirculation in both cases. For the bluff-body, the vorticity is create by the sidewall boundary layer, and for the swirl, the source of vorticity involves a mechanism that they labeled as conversion of axial vorticity into azimuthal vorticity, caused by the bending of vortex filaments. Anacleto (1993) made a experimental study of a LPP combustion chamber, presenting temperature measures in order to see the results of premixing of the reactants. It was observed by him that the premixing allow the burning of liquid fuel to lower flame temperatures, reducing the pollutants.

In the present work simulations of the LPP combustion chamber is performed using the CFX 5.5.1 comercial software, considering for a first analysis the isothermal flow. The numerical results will show the velocity field with vectors and streamlines. The simulation is going to be steady and unsteady state to observe the evolution on time of the flow inside the chamber. The behavior of the recirculation zone behind the bluff body, with and without swirl is going to be the focus of the discussion. This paper will investigate the effectivness of the $k-\epsilon$ model for this simulation because, although this model is very used in industrial flow, it can overestimate the shear stresses in certain cases, due to its formulating of the production term of turbulent kinetic energy.

The simulation was first performed for a test case studied by Taylor and Whitelaw (1984). This previous work provides a lot of experimental results that were used for the validation of the present strategies of simulation. After that, the flow is simulated for the LEA-LPP combustion chamber considering different levels of swirled flows.

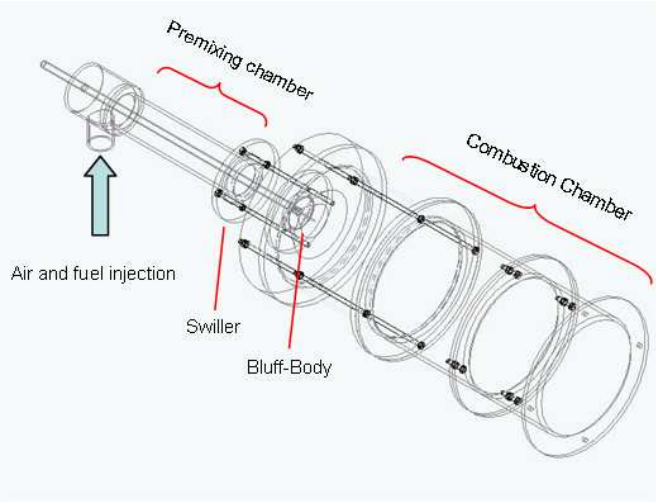

Figure 1: LEA-LPP Combustion Chamber

2. Mathematical Modelling

2.1 Governing Equations

For incompressible turbulent flows, the conservation of mass, and momentum can be expressed by the classical Reynolds averaged equations given by:

$$\nabla.\mathbf{U} = 0 \tag{1}$$

$$\frac{\partial \mathbf{U}}{\partial t} + (\nabla \mathbf{U})\mathbf{U} = -\frac{1}{\rho}\nabla P + \nabla.(\nu \nabla \mathbf{U} - \overline{\mathbf{u} \otimes \mathbf{u}}) \tag{2}$$

In those equations $\mathbf{U}$, P are the mean velocity and pressure fields; ρ, ν are the density and kinematics viscosity of the fluid; and $\overline{\mathbf{u} \otimes \mathbf{u}}$ is the Reynolds stress tensor modeled by the Boussinesq eddy viscosity

assumption:

$$\overline{\mathbf{u} \otimes \mathbf{u}} = \frac{2}{3}k\mathbf{I} - 2\nu_T \mathbf{D}(\mathbf{U}) \tag{3}$$

where ν_T is the turbulent eddy viscosity, $\mathbf{D}(\mathbf{U})$ is the mean rate-of-strain tensor, $\mathbf{I}$ is the identity tensor and k the kinetic energy of turbulence.

The turbulent eddy viscosity is modeled by the Prandtl-Kolmogorov relation written as:

$$\nu_T = C_\mu \frac{k^2}{\epsilon} \tag{4}$$

where ϵ is the dissipation rate of kinetic energy. It is the basis of the classical k-ϵ model of turbulence. This model requires the use of two additional transport equations for k and ϵ given by:

$$\frac{\partial k}{\partial t} + \mathbf{U}.\nabla k = \nabla.\left[(\nu + \frac{\nu_T}{\sigma_k})\nabla k\right] + P_k - \epsilon \tag{5}$$

$$\frac{\partial \epsilon}{\partial t} + \mathbf{U}.\nabla \epsilon = \nabla.\left[(\nu + \frac{\nu_T}{\sigma_\epsilon})\nabla \epsilon\right] + C_{\epsilon 1} P_k \frac{\epsilon}{k} - C_{\epsilon 2}\frac{\epsilon^2}{k} \tag{6}$$

In those equations P_k is the production of k which is written as:

$$P_k = 2\nu_T \left[\mathbf{D}(\mathbf{U}) : \mathbf{D}(\mathbf{U})\right] \tag{7}$$

The standard values of the constants were proposed by Jones and Launder(1972), given as follows:

$$C_\mu = 0.09; C_{\epsilon 1} = 1.44; C_{\epsilon 2} = 1.92; \sigma_k = 1.0; \sigma_\epsilon = 1.3$$

2.2 Boundary conditions

For inflow surfaces the values of velocity, kinetic energy of turbulence and dissipation fields are prescribed. For outflow boundaries the homogeneous Neumman conditions are prescribed for the same variables and the homogeneous Dirichlet boundary condition is used for the pressure field.

Close to solid boundaries the turbulence model, as presented in 1 - 2, does not hold. The computational domain have to be dislocated at a distance δ from the solid walls and equilibrium laws such as the classical log-law for mean velocity are imposed for the parallel surface. In this surface the local components of the velocity field are prescribed as:

$$\mathbf{U}.\mathbf{n} = 0 \ ; \ \mathbf{U}.\mathbf{s} = 0 \tag{8}$$

and :

$$\frac{\mathbf{U}.\mathbf{t}}{u_f} = \begin{cases} \frac{\delta u_f}{\nu}; & \text{if } \frac{\delta u_f}{\nu} \leq 11.5 \\ \frac{1}{\kappa}\ln\frac{\delta u_f}{\nu} + C; & \text{if } \frac{\delta u_f}{\nu} > 11.5 \end{cases} \tag{9}$$

This boundary condition introduces the constants κ and C, and the friction velocity which is calculated by:

$$u_f^2 = (\nu + \nu_T)\frac{\partial}{\partial n}(\mathbf{U}.\mathbf{t}) \tag{10}$$

The unit vectors $\mathbf{n}, \mathbf{t}$ and $\mathbf{s}$ compose a local frame deduced from the normal and tangential directions of the near wall streamlines.

For k and ϵ, the boundary conditions are obtained considering the balance of production and dissipation at the surface located on δ. So, the k equation leads to the Dirichlet boundary conditions:

$$k = \frac{u_f^2}{\sqrt{C_\mu}} \ ; \ \epsilon = \frac{u_f^3}{\kappa\delta} \tag{11}$$

3. Computational details

The flows analyzed in the present paper were simulated using the commercial software CFX 5.5.1, with the standard $k - \epsilon$ model of turbulence and log-law, as described in the previous chapter.

In order to make a simulation of a LPP chamber, it is necessary first to check the reliability of the turbulence model for the simulation of this kind of recirculating flow. For this purpose, a similar test case will be studied, concerning a flow around a bluff-body. The experimental work of Taylor and Whitelaw (1984) for a bluff-body in the shape of a disk with 25% of blockage area were analyzed (Fig. 2). This is a good test case and a lot of experimental data that can be used to verify the behavior of the $k-\epsilon$ for this kind of flow. An important point to be highlighted is that the choice this simple model is justified considering future computations of the reactive flow on the proposed combustion chamber geometry. The turbulence models for reactive flows, in particular for combustion flows, is implemented only for simple models of turbulence. The use of $k-\epsilon$ of turbulence is then a natural choice for a less expensive analysis of the complete problem considering complex features as combustion and heat transfer by radiation.

The experimental measurements of radial velocity in successive axial stations will be compared with the numerical results. The bluff-body has a disk diameter of 25.4mm and a thickness of 2.67mm. The bluff's shaft diameter is 6.4mm and its length is 224mm, as shown in the Fig. 2. The bluff-body was positioned inside a water flow in a duct with 50.3mm of diameter. The origin of the axial and radial coordinates is taken, as if the experimental work, at the center downstream of the bluff-body. The inlet boundary condition was set to obtain a Reynolds Number of 34700. This simulation was performed in steady state, with a mesh refinement at the surroundings upstream and downstream of the face of the bluff-body. The radial profiles of axial velocity will be plotted and compared with the correspondent experimental data. The positions are given as follows: 1. -0,84R; 2. -0,20R; 3. 0,02R; 4. 0,20R; 5. 0,40R; 6. 0,60R; 7. 0,80R; 8. 1,19R; 9. 1,59R; 10. 1,99R; 11.2,39R; 12. 3,18R; 13. 4,38R; 14. 5,97R. (Fig. 2b) Six of those positions are going to be chosen to compare with experimental data.

Figure 3 shows the unstructured mesh used in the computations. Is is a discretization of the entire domain and the symmetry was not considered in order to analyze the possibility of occurrence of unsteady flow. The mesh uses 236661 nodes and 1329739 elements (tetrahedron). To improve the results near the wall in some of the axial positions, the CFX's inflation boundary resource was used. The time step for the computation was chosen as 10^{-2} sec and the convergence tolerance was set as 10^{-5} in RMS value of all fields norm.

For the simulations of the LEA-LPP combustion chamber, a mesh with 231818 nodes and 1309474 elements was used (Fig. 4). The same density of spatial dicretization for the test case 1 is used. The same values of time step and convergence limiter are also used.

For this case the flow in the chamber is 24 l/s and the swirl number is chosen as 0.0 or 0.03. Three axial positions of the bluff-body were simulated in order to determine the recirculation regions in different points of operation of the combustion chamber.

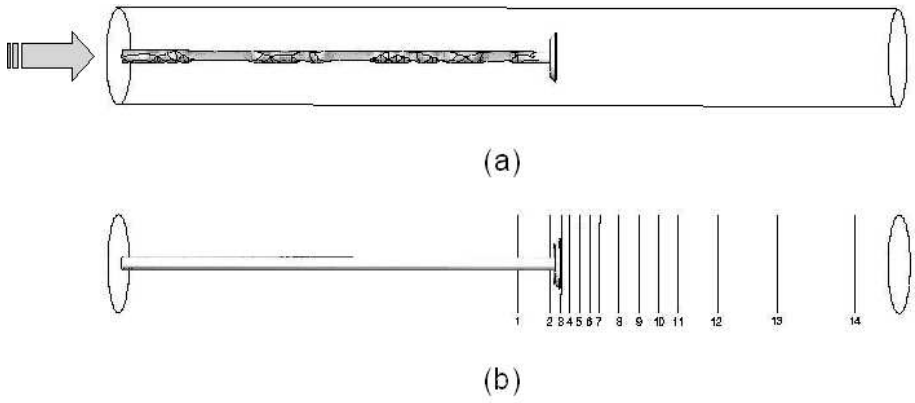

Figure 2: (a) Confined Disc Bluff geometry (b) Position of Experimental Data

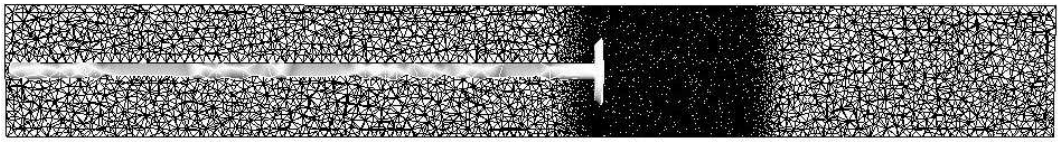

Figure 3: Confined Disc Bluff: Unstructured Computational Mesh

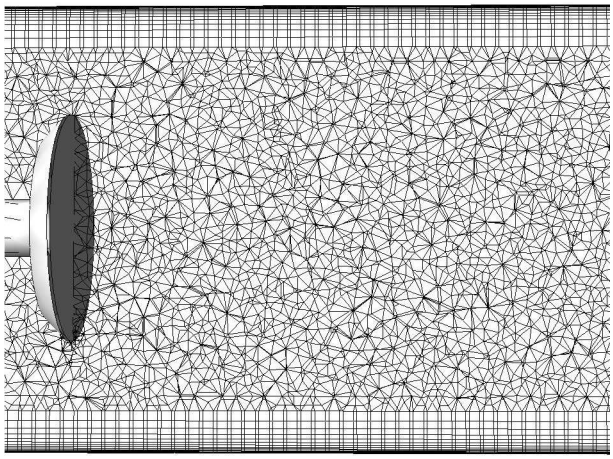

Figure 4: Confined Disc Bluff: Refinement and inflation detail

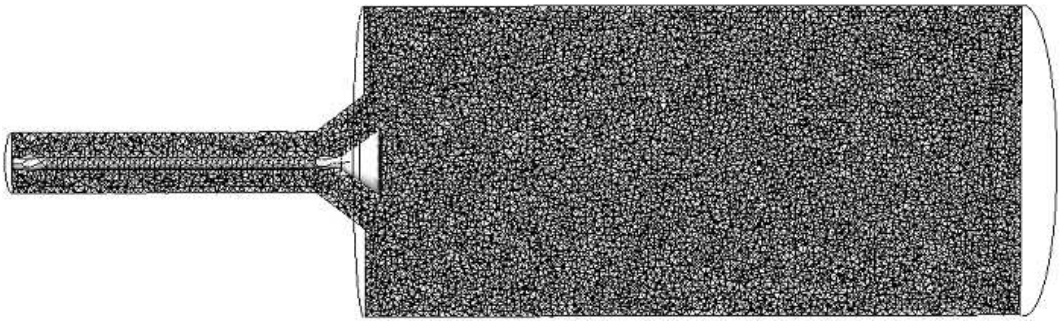

Figure 5: LEA-LPP Combustion Chamber: Unstructured Computational Mesh

4. Results and Discussions

The results for the test case 1 (Confined Disc Bluff) are presented in the figures 6 and 8. The velocity plot is presented in the figure 6, where the recirculation region can be observed. The flow is accelerated in the area blockage confining the recirculation region behind the disc. The velocity display obtained is in agreement with the experimental results, because the recirculation length obtained in the simulation is approximately 4cm, or in bluff's diameter, 1,57D. The experimental result is 4.4cm, or in bluff's diameter, 1,75D. The relative error between the simulation and the experimental results is approximately 10%. Based on that, the simulation can be considered as good. The graphical analysis also shown in the figure presents a good proximity between the simulation and the experimental results. The six axial positions that were chosen to compare and analyze the results. It can be seen that the best results happens at the surroundings of the bluff, more precisely at -0,20R, 0,20R and 0,60R profiles. This indicates that the $k-\epsilon$ model were able to predict the flow in this region. Other models can also be very accurate at other regions, like, for example, the $k-\omega$ model can be very precise to analyze the separation flow at the tip of the bluff-body, and the Reynolds stress model can be very good at the ending of the recirculation zone, because this model is indicated for flows which has strong streamline curvature, which is the case of swirling simulations.

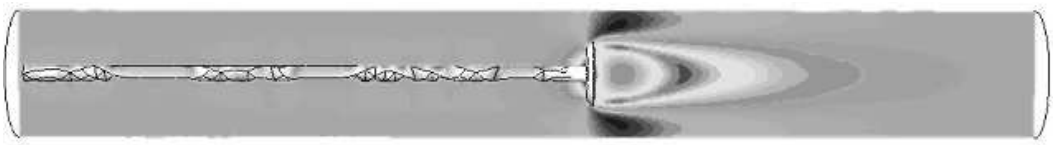

Figure 6: Confined Disc Bluff: Axial velocity levels

In the no-swirling case, the simulation for the position 0 shows the beginning of a three-dimensional vortex shedding phenomenon. It resembles the results obtained by Huang and Tsai, for a bluff-body-effect-dominated regime. Although their results are for a swirling flow, the comparing is valid, due to the fact that this type

Figure 7: Confined Disc Bluff: Visualization of recirculation zone

of regime is dominated by the bluff-body with low swirl numbers. The shedding isn't going longer than the shedding obtained by them, but the first two vorticities are very similar, and the shedding obtained is due to the fact that the position of the bluff-body is a little bit far from the diffuser, which is against of a good flame holding. For the positions 1 and 2, there are axissymetric vorticities, but in the position 2, the vorticities are a little bit narrower than the position 1, which resembles and accord with the result obtained by Taylor and Whitelaw. In the beginning, for the position 1, the vortexes start behind the bluff-body, and finish at the chamber´s boundary with the vortexes coming and going with the time running. The vortex breakdown in this position occurs in the halfway of the chamber, which resembles the work of Anacleto, who made a visual observation of the flame in a LPP combustion chamber, and obtained a flame who is holded in the halfway of the chamber too. For the position 2, in the beginning, there is a double vortex shedding, then, happens the same vortex motion that were observed in position 1 with the continuing of the vortex shedding. This time, the vortex breakdown isn't happening, which shows that this position is against of a good flame holding too, as in position 0. The simulation for this case has, for almost all global balances, maximum residual errors of the order of 10^{-3}, which, according to the CFX manual books, is the indication of a reasonable level of convergence, good enough to engineering applications, and with percentual errors being probably below 0.5%. But some errors are a little bit above this valor, which can indicates some of the flaws of the turbulence model. The errors could been happening in equations there aren't influenced by the pressure field, and physically, the errors can occur at the surroundings of the diffuser, because the $k-\epsilon$ model had the tendency to overestimate the shear stress and to underestimate the separation zone. So, although there are very noticeable vorticities, a few of them could not been shown, due to this flaw.

For the swirling case it can be seen that the swirling wake is present in positions 0 and 1, which accords with the results of Huang and Tsai(2001). In position 0, it can be seen the presence of a reverse flow region inside the diffuser, which happens in large swirl numbers at the jet exit. In the 0 and 1 positions a annular vortex appears. All this patterns varies with the swirl number, which isn't happening in this simulation. So, the change of patterns can be credited to the position changing of the bluff-body. In the positions 0 and 1, the streamlines show the beginning of a attachment right after the diffuser, which is countered by the swirling wake. There isn't much transient phenomena at positions 0 and 1. In this case, it can be said that the $k-\epsilon$ model shows good results, due to the fact that a lot of experimental results were identified in the simulation. But, even in swirling simulations, the model can have the same deficiencies described in the no-swirling case. In the other hand, the simulation in this case has maximum global balance residual errors in the order of 10^{-3}, which indicates a good convergence level. In this case, there were no errors below this valor, so, probably, the simulation was well succeeded. For both cases, it can be seen that the position 1 is going to be the best position for a good flame holding.

For the LPP chamber simulation, the recirculation length was calculated and for the no-swirling case, the position 1 shows a length of 20,5cm, or in bluff's diameter, 0,21D. For the position 2, the length is 0,113cm or, in bluff's diameter, 0,21D. In the swirling case, the results are very close, with 0,125cm for position 0 and 0,123 for position 1. In bluff's diameter, the result is 0,2315D and 0,23D respectively. The results for both cases confirm the visual observation that was made above. It must be noted that the test simulation was made in steady state, and this simulation was made in transient state so, excepting for position 0 in the no-swirling case the results obtained here are ending in an axisymmetric flow. The position 0 is the exception is because of the vortex shedding that happens due to the position of the bluff-body.

5.Conclusions

There were presented results of a numerical simulation of a isothermal flow inside a LPP combustion chamber, and its results were compared with experimental results of similar flows.To check the reliability of the turbulence model, a test simulation with experimental results was conducted first.

The results of the validation case were compared with their experimental correspondent of axial velocity profiles and recirculation zone length. The graphical analysis of the axial profiles shows good agreement with the experimental data at the surroundings of the bluff-body, and the recirculation length obtained in the simulation is near the experimental result, with a relative error of 10%. For the LPP simulation, in the no-swirling case, the position 0 shows a vortex shedding, and the positions 1 and 2 shows axisymmetric flows, with narrower vorticities for position 2, due to the increased blockage of the flow. Some of the maximum global balance errors in this case are a little bit above the ideal valor that is recommended by the CFX manual books. For the swirling case, the results had shown a change of flow pattern with the position change of the bluff-body. The position 0 shows a reverse flow inside the diffuser, that happens because the position of the bluff-body. Both of the positions shows a annular vortex and a beginning of a attachment after the diffuser, countered by the swirling wake, present in both positions. The position 2 in the swirling case wasn't shown because, for the swirling case, this position is very extreme and, it won't provide a good flame holding. Here, all the maximum global balance errors are below the recommended by the CFX manual books. Based on this results, the best position for the bluff-body is the position 1.

Finally, the conclusion is that the results obtained here can be considered as good, but only experimentation can validate the results. A possibility in the future is making use of other methods of numerical simulation, such as LES (large-eddy simulation) or DNS (direct numerical simulation) for the LPP case, if a machine capable of running this type of simulation exists.

6.Acknowledgments

Support for this research has been provided by ELETRONORTE - Centrais Elétricas do Norte do Brasil S.A., and CNPQ's energy fund, under the process $103543/2002 - 3$.

6. References

Anacleto, P. J. S. M., 1993, "Análise Experimental de uma Câmara de Combustão Axissimétrica com Pré-Vaporização e Pré-Mistura de Reagentes" Master degree dissertation. IST-Lisbone.

Chen, R. H., Driscoll, J. F., Kelly, J., Namazian, M., Schefer, R. W., 1990 "A Comparision of Bluff-Body and Swirl-Stabilized Flames", Combust. Sci. And Tech., Vol.71, pp 197-217

Chigier, N.A., Beér, J.M, 1964, "Velocity and static pressure distribution in swirling air jet issuing from annular and divergent nozzle", ASME Journal Basic Eng., 86, pp. 788-796.

Huang, R. F., Tsai, F. C., 2001, "Observations of Swirling Flows Behind Circular Disks", AIAA Journal, Vol. 39, No. 6 pp. 1106-1112

Koutmos, P., McGuirk, J. J., 1991, "Isothermal Modeling of Gas Turbine Combustors: Computational Study", J. Propulsion, Vol. 7. No. 6, pp. 1064-1071

Schefer, R. W., Namazian, M., Kelly, J., 1994, "Velocity Measurements in Turbulent Bluff-Body Stabilized Flows", AIAA Journal, Vol. 32, No. 9 pp. 1844-1851

Sheen, H. J., Chen, W. J., Jeng, S. Y., 1996, "Recirculation Zones of Unconfined and Confined Annular Swirling Jets", AIAA Journal., Vol.34, No. 3. pp. 572-579

Taylor, A. M. K. P., Whitelaw, J.H., 1984, "Velocity Characteristics in the Turbulent Near Wakes of Confined Axissymetric Bluff Bodies", J. Fluid Mech., Vol.129, pp. 391-416.

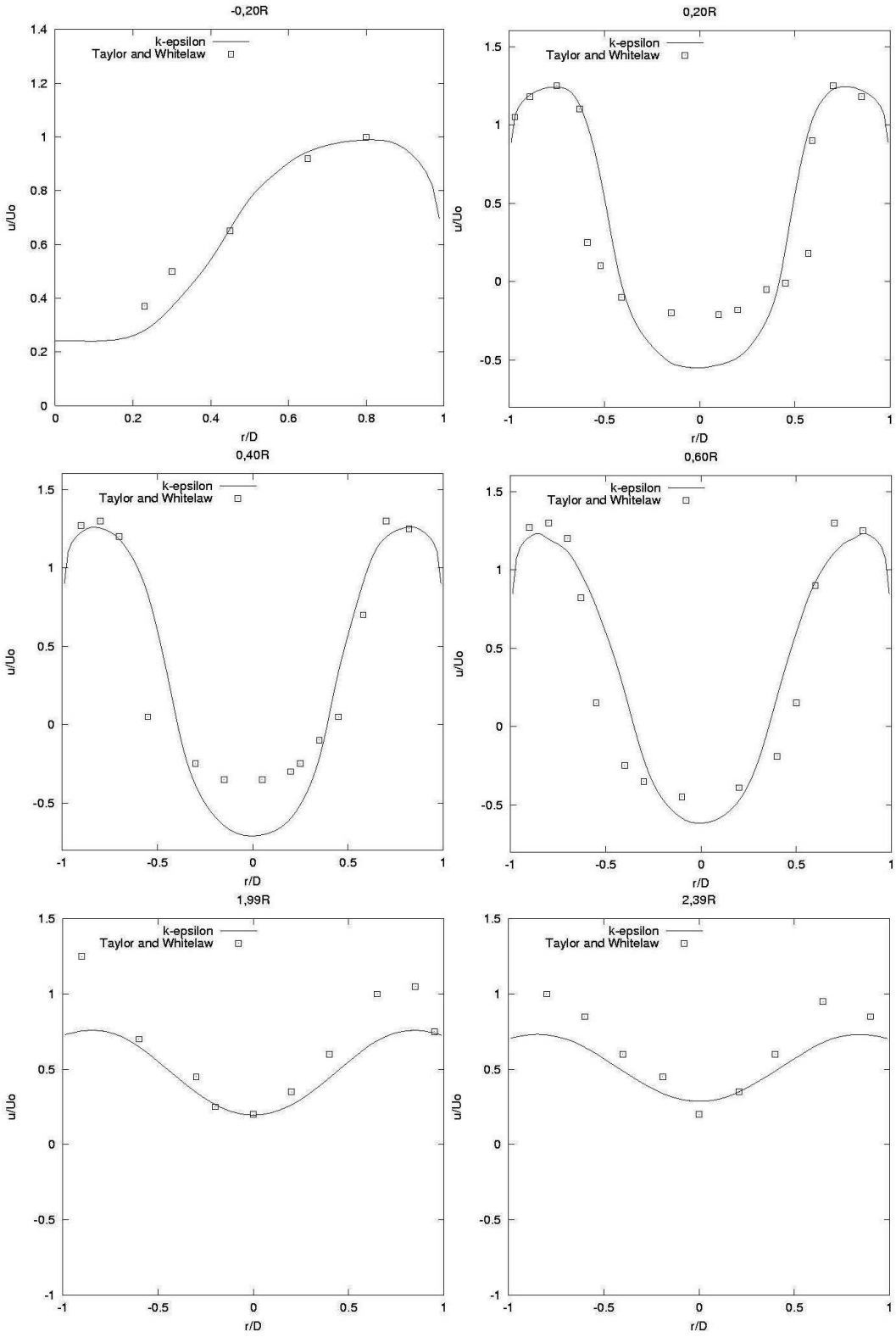

Figure 8: Confined Disc Bluff: Velocity profiles

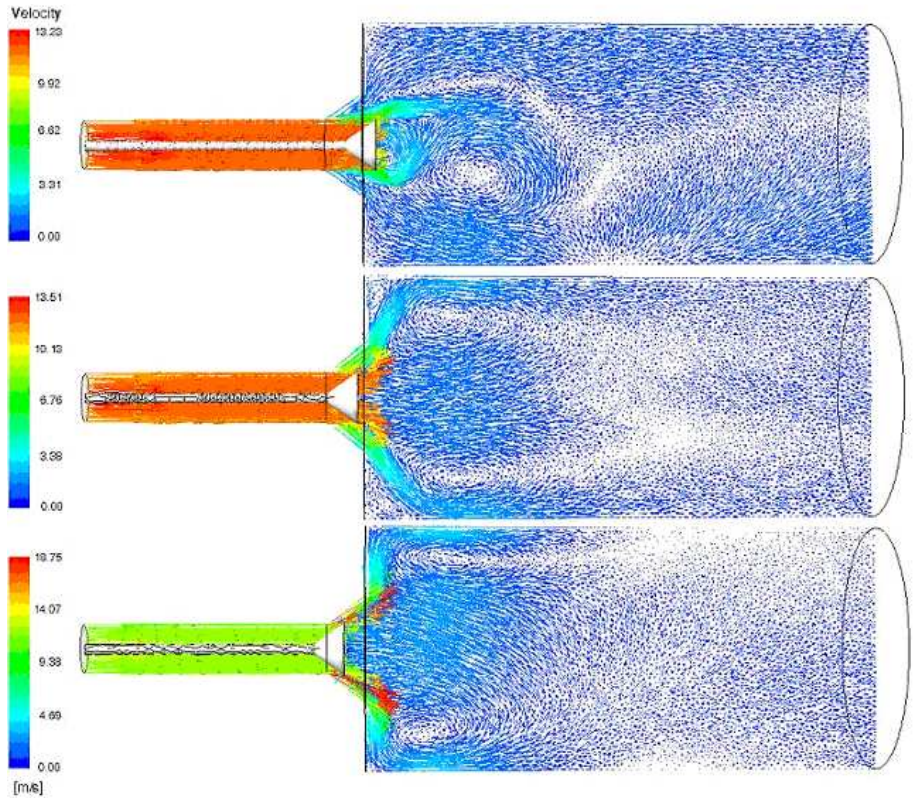

Figure 9: LEA-LPP Combustion Chamber: Velocity plots for no-swirl simulations

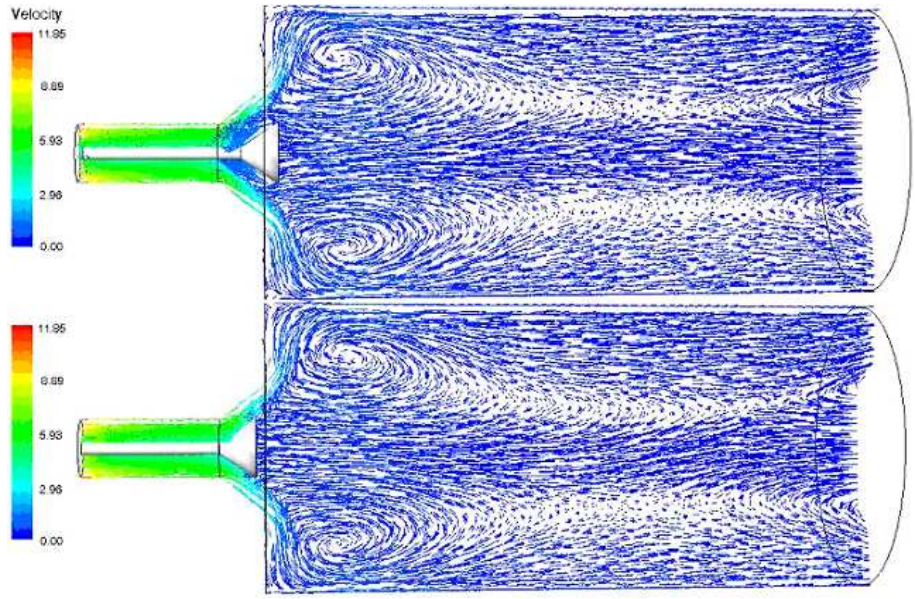

Figure 10: LEA-LPP Combustion Chamber: Velocity plots for simulations with swirl

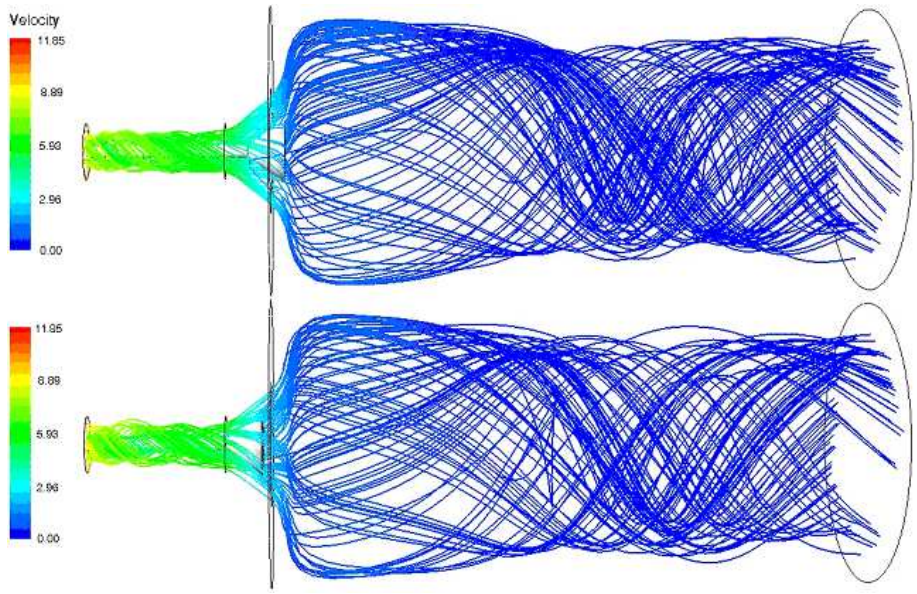

Figure 11: LEA-LPP Combustion Chamber: Streamlines for simulations with swirl

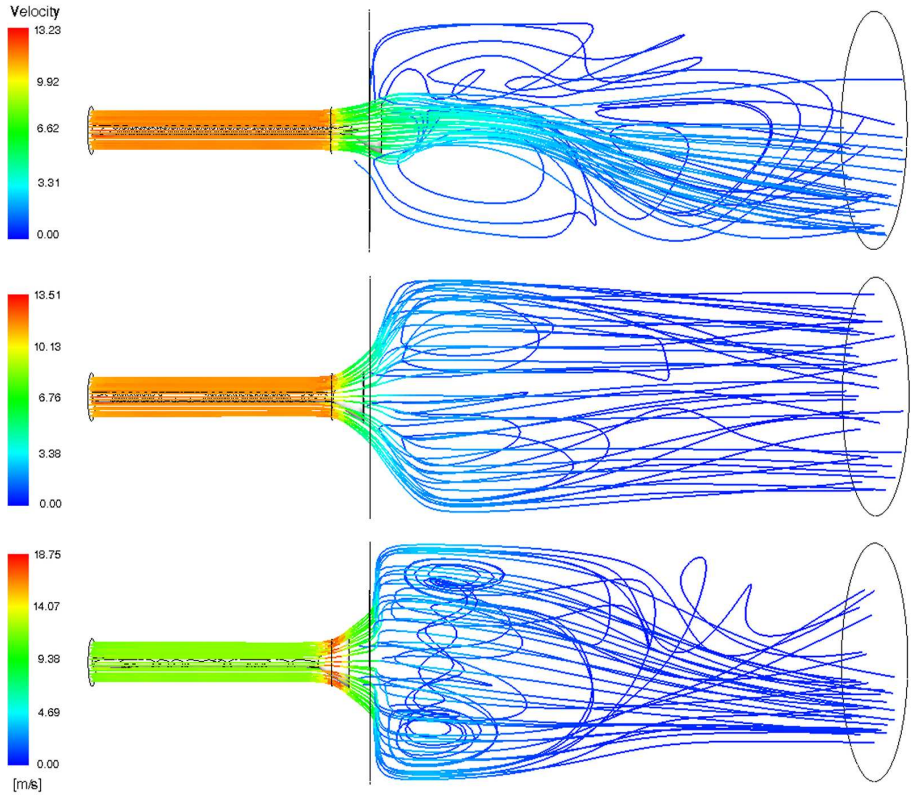

Figure 12: LEA-LPP Combustion Chamber: Streamlines for no-swirl simulations